sciendo

Polish Journal of Chemical Technology, 26, 4, 17—24, 10.2478/pjct-2024-0035

Sodium Metasilicate-MgO Blend Catalyst for Producing Mono and Diacylglycerol from Palm Kernel Oil Using High Shear Compartment Reactor

Arief Rakhman Affandi[1, 2], Ria Millati[1], Chusnul Hidayat[1*]

[1]Department of Food and Agricultural Product Technology, Faculty of Agricultural Technology, Universitas Gadjah Mada, Jl. Flora No 1 Bulaksumur, Yogyakarta, Indonesia
[2]Permanent Address: Department of Food Technology, Universitas PGRI Semarang, Jl. Sidodadi Timur No. 24 Semarang, Indonesia
[*]*Corresponding author:* e-mail: chusnulhi@ugm.ac.id

Sodium metasilicate (SMS) tended to agglomerate during glycerolysis reactions in high shear compartment reactors (HSCR), hindering triacylglycerol (TAG) conversion. Therefore, the aim was to evaluate the SMS-magnesium oxide (MgO) blend as a heterogeneous catalyst for glycerolysis reactions. Various SMS-MgO ratios (ranging from 2.5:1 to 10.0:1) were evaluated. The results demonstrated that increasing MgO in the blend reduced catalyst basicity and minimized O-Si-O groups and catalyst crystallinity, preventing clumping and increasing catalyst surface area. The SMS-MgO 5.0:1 blend exhibited the smallest pore size (<2 nm) with a surface area of 4.22 $m^2 \cdot g^{-1}$ and basicity of 11.59 ± 0.115 $mmol \cdot g^{-1}$. This blend achieved the highest TAG conversion of 53.98%, with a MAG content of 16.86 ± 0.528% when it was performed at 120 °C with an agitator speed of 2,000 rpm for 6 h. Thus, the SMS-MgO 5.0:1 blend shows promise as a heterogeneous catalyst in glycerolysis reaction in HSCR, hindering agglomeration and enhancing surface area.

Keywords: Basicity; Catalyst Agglomeration; Glycerolysis; High Shear Compartment Reactor; MgO-Sodium metasilicate blend.

INTRODUCTION

A mixture of Monoacylglycerol (MAG) and diacylglycerol (DAG), also called MDAG, are additives widely used in food and non-food products and are classified as GRAS non-ionic emulsifiers. This type of emulsifier is produced through various chemical[1, 2] and enzymatic processes[3, 4]. A homogeneous catalyst, such as NaOH or KOH, is commonly used in the glycerolysis reaction, such as MAG and DAG synthesis from Refined Bleached Deodorized (RBD) Stearin[5]. Interesterification reactions can also utilize organocatalysts alongside homogeneous catalysts, broadening the scope of catalyst options available for this process[6, 7]. However, homogeneous catalysts and organocatalysts have several drawbacks. The homogeneous catalyst can only be used once, and the residues have to be separated from the product[8]. The limited scalability associated with organocatalysts poses challenges in their widespread application in interesterification reactions[9]. On the other hand, heterogeneous catalysts are a solid form of catalyst that has been investigated by several researchers in this reaction, causing the process of interesterification cost-efficient[10–12]. Currently, many different kinds of heterogeneous catalysts, such as MgO[2, 13], zinc glycerolate[1], and sodium silicate[14], have been used extensively in interesterification processes, such as in the manufacture of biodiesel[15–17], glycerol carbonate[18–20], and mono and diacylglycerol[3, 21].

Both SMS and MgO have great potential to be used in the interesterification process due to their strong alkalinity[13, 14, 22–24]. However, several researchers have reported experiencing difficulties in applying this catalyst in its non-calcined form, especially for sodium metasilicate. It is possible due to the hydrolysis process of non-calcined sodium silicate, which forms H_4SiO_4 monomers. This reaction caused the solid catalyst agglomeration, influenced mass transfer, and reduced trans-esterification product yield[25]. The forming of SiO_4 bridges on the catalyst can be prevented by mixing the catalyst with other oxide materials, which also improves the solid base catalyst's ability to be reused[22].

One significant drawback of the glycerolysis reaction is the immiscibility of glycerol with oil. This lack of compatibility between the two substances leads to difficulties in mixing them efficiently. As a result, the mass transfer between glycerol and oil becomes limited, hindering the overall effectiveness and efficiency of the reaction. To solve this issue, tert-butanol and tert-pentanol were used as solvents[8]. Ultrasonication and high shear reactor were also used to enhance the mass transfer rate[26]. Forming an emulsion system with a very small globule particle size improved the mass transfer. The catalyst's surface will react with the globules efficiently due to their small size, increasing the reaction rate. However, high shear can damage solid catalysts, resulting in a change in their properties and a decrease in their overall efficacy[27]. To overcome this problem, a compartment has been incorporated into the high shear compartment reactor (HSCR) to protect the catalyst from damage by the impeller. A combination of compartments and high-speed agitation was performed to deal with the miscibility of the substrate. Therefore, this study evaluated the use of a high-alkalinity solid base catalyst based on a mixture of uncalcined sodium metasilicate and magnesium oxide (MgO) to synthesize mono- and diacylglycerol using HSCR. The effect of SMS and MgO blend on its efficacy, including catalyst basicity, crystallinity, surface area, pore volume, and performance in the glycerolysis process, was investigated. An HSCR was employed to create a homogenous substrate and identify catalyst property changes.

MATERIALS AND METHODS

Materials

Refined bleached deodorized palm kernel oil (RBDPKO) was obtained from PT Smart Tbk (Bekasi, Indonesia). Sodium metasilicate (SMS) (Na_2SiO_3) was obtained from Sigma–Aldrich (Missouri, USA), and magnesium oxide (MgO) powder was obtained from Merck KGaA (Darmstadt, Germany). Glycerol was obtained from P&G Chemicals (Kuala Lumpur, Malaysia). The Silica Gel 60 F254 TLC plate was obtained from Supelco Merck (Darmstadt, Germany).

Catalyst Preparation

Wet impregnation of the MgO was carried out by heating 30 g of MgO in 150 mL of distilled water. The mixture was then heated for 2 h at 80 °C. After filtration, The MgO slurry was dried and crushed to a fineness of mesh 100. Anhydrous sodium metasilicate (SMS) and MgO were mixed in the following ratios: 2.5:1 (SMS--MgO 2.5:1), 5.0:1 (SMS-MgO 5.0:1), 7.5:1 (SMS-MgO 7.5:1), and 10.0:1 (SMS-MgO 10.0:1). The powder mixture was mixed with 5% (wt) of distilled water, and the slurry was dried at 105 °C for 6 h. The dried catalyst was crushed to pass through mesh 15 but remained in mesh 30, resulting in catalyst granules.

Glycerolysis Reaction in High Shear Compartment Reactor

The process of glycerolysis was carried out with a mole ratio of RBDPKO and glycerol equal to 1:3. The substrate mixture was heated to 120 °C. The catalyst concentration was 20% (based on the oil mass), with the catalyst granule placed in the reactor compartment (Figure 1). The reaction was performed for 6 h at an agitation speed of 2000 rpm. Every 60 min, a sample was collected.

After the reaction, the catalyst was removed from the compartment. A washing process was carried out using a mixture of n-hexane and ethanol[28]. The previously used catalyst granules were added to the solution and stirred for 30 minutes in a 1:1 (v/v) mixture of hexane and ethanol, with a total volume of 50 mL. A new solution was used to wash the granules of the catalyst after the first wash. The granules were dried for 2 h at 105 °C to eliminate any remaining solution. Finally, TLC was used to examine MAG, DAG, and TAG concentrations.

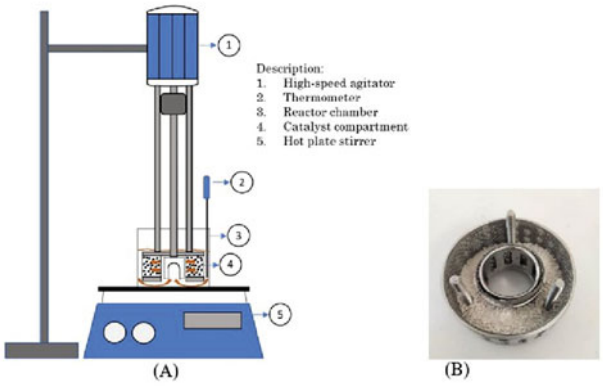

Figure 1. (A) High-shear reactor design for the glycerolysis reaction; (B) compartment filled with heterogeneous catalyst

Characterization of Sodium Metasilicate and MgO Blend Catalyst

NOVAtouch Lx4 (Quantachrome Instruments, Graz, Austria) was used to analyze the pore size and pore volume of the catalyst using N_2 gas sorption. The isotherms for adsorption and desorption were determined using the multipoint approach. The Brunauer, Emmett, and Teller (BET) technique was used to determine the total surface areas[29]. The Barrett-Joyner-Halenda (BJH) method provided mesoporous size distribution[30]. The benzoic acid titration method was used to determine the basicity of the solid catalyst[31].

Fourier Transform Infrared Analysis

The Fourier Transform Infrared (FTIR) method was used to determine the functional groups of the catalyst granules, which was carried out using Perkin Elmer UATR (USA). X-ray diffraction (XRD) analysis was carried out using a Shimadzu XRD 7000 S/L (Japan) with Cu radiation (30 kV and 30 mA). The samples were scanned in the range of $2\theta = 10–90^{o}$ at a scanning speed of 4^{o}/min.

Analysis of Fatty Acid and Acylglycerols Composition

Gas chromatography (GC-2010 Shimadzu, Japan), outfitted with a flame ionization detector and a silica capillary column DB 23 (Agilent, USA), was used to examine the fatty acid content of triacylglycerol in RBDPKO. The retention time was used to determine the presence of fatty acids, which were then compared to standards of FAME (Sigma-Aldrich, USA), and the results were reported as a percentage of fatty acids. The amount of free fatty acids was calculated using the titration method described in AOCS Ca 5a-40[32].

Thin Layer Chromatography (TLC) was used to determine acylglycerol compositions (mono–, diacylglycerol, and triglyceride) in the raw material of RBDPKO and the product of the glycerolysis process[33]. One μL of the sample was spotted on a TLC plate that had been dried at 105 °C for 1 h. The mobile phase for elution was hexane: ethyl ether: glacial acetic acid (80:20:2) (v/v/v). After the chamber had been filled with the mobile phase, the TLC plate was put in the chamber. The TLC plate remained upright within the chamber until the mobile phase (eluent) reached the finish line, located 1 cm from the plate top. When the elution process was completed, the plate was removed from the chamber and allowed to dry at ambient temperature. Coloring of the TLC plate was accomplished by employing Coomassie brilliant blue at a concentration of 0.02% (w/v), which has been dissolved in a mixture of acetic acid, methanol, and distilled water in the proportions of 1:3:6 (v/v/v)[5]. Camag's Automatic TLC Scanner III S/N (1.14.16) was used to scan the TLC plate at a wavelength of 629 nm, and WinCATS software was used to analyze the data. The scanner software integrates the signal intensity for each spot. This integration gives a peak area, which is proportional to the amount of the compound. By comparing all of the peak areas of sample, the software can calculate the concentration of MAG (Eq. 1), DAG (Eq. 2), and TAG (Eq.3) in the sample.

$$\text{MAG Concentration (\%)} = \frac{\text{Peak areas of MAG}}{\text{Total peak area}} \times 100\% \quad (1)$$

$$\text{DAG Concentration (\%)} = \frac{\text{Peak areas of DAG}}{\text{Total peak area}} \times 100\% \quad (2)$$

$$\text{TAG Concentration (\%)} = \frac{\text{Peak areas of TAG}}{\text{Total peak area}} \times 100\% \quad (3)$$

The TAG conversion formula is shown in Equation 4:

$$\text{TAG Conversion (\%)} = \frac{\text{TAG}_0 - \text{TAG}_t}{\text{TAG}_0} \text{x } 100\% \quad (4)$$

where subscript 0 and t are the starting and final concentrations, respectively.

Analysis of Water Content and Slip Melting Point

Water content and slip melting point were determined by Karl-Fisher titration (AOCS Ca 2e-84) and AOCS Cc 3b-92, respectively.

Statistical Analysis

The statistical analysis was performed using an SPSS 26.0.0 (SPSS Inc., USA) program. Tuckey's multiple comparison tests were used to compare mean values and differences among mean values were considered significant when $P < 0.05$.

RESULTS AND DISCUSSION

Characteristics of RBD Palm Kernel Oil

The fatty acid profile, free fatty acid value, water content, and slip melting point of RBDPKO are presented in Table 1. The result showed that RBDPKO's fatty acid composition was dominated by lauric acid, which accounted for 47.24% of the total. Kılıç & Özer found nearly the same number of 47.74% in their study[34]. As a result, RBDPKO exhibits a high slip melting point value, typically around 23 to 26 °C. This melting point characteristic makes it ideal for applications where solid fats are required, such as in the production of confectionery, emulsifiers, and cosmetic formulations.

Effect of SMS-MgO Mass Ratio on Functional Groups of Catalyst

FTIR analysis was used to characterize the functional groups of the catalyst. The IR spectra of the catalyst at various SMS-MgO ratios were evaluated in the range of 450–4000 cm^{-1}. Figure 2 shows that the spectra displayed an absorption band at a frequency of ~969 cm^{-1}, which was interpreted to be caused by the stretching of Si-O-Na[14, 25]. The appearance of Si-O-Si stretching bands at approximately 827 cm^{-1} was ascribed to tetrahedral SiO_4^{4-} aggregation, which consequently formed Si-O-Si[31]. The observed bands with a wavenumber of 702 and 1165 cm^{-1} indicated the stretching vibrations of Si-O bonds[35, 36]. The catalyst surface exhibits the presence of various carbonate species (O-C-O) at a wavenumber of 1441 cm^{-1} [37]. This occurrence can be attributed to the catalyst's alkaline properties and its interaction with atmospheric CO_2. The spectral peaks observed at wavenumbers 515 and 871 cm^{-1} are attributed to the distinct modes of the stretching vibration involving the O-Si-O bonds[36]. The observed decrease in peak intensity at this specific wavelength on the SMS-MgO (2.5:1) catalyst may be attributed to the presence of MgO particles that are adhered to the surface of the sodium metasilicate granules. This attachment potentially hinders the formation of O-Si-O bonds. Thus, it minimized catalyst agglomeration.

In the process of impregnation, it is widely known that the reaction of MgO with distilled water will result in the formation of a molecule of magnesium hydroxide ($Mg(OH)_2$). A peak at 2927 and 3693 cm^{-1} can be attributed to the residual C-H bond and vibrational stretching of hydroxyl (OH) groups inside the catalyst compound, respectively[35, 38, 39]. The observed peak at a wavenumber of 777 cm^{-1} is attributed to the stretching vibration of Mg-O-Mg[40]. In addition, an absorption peak is observed at around 458 cm^{-1}, which can be attributed to the vibrations of the Mg–O bond[41]. An increase in the peak at this wavelength was observed as a result of employing a greater quantity of MgO powder in the catalyst mixture.

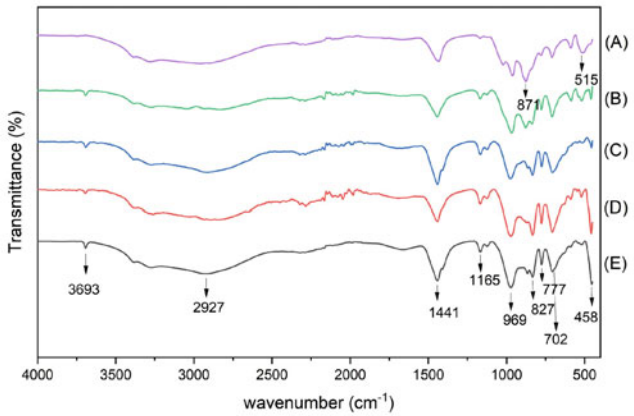

Figure 2. FTIR spectrum of sodium metasilicate (SMS) to magnesium oxide (MgO) ratios. SMS-MgO ratios were 1:0 (A); 10.0:1 (B); 7.5:1 (C); 5.0:1 (D); and 2.5:1 (E)

Table 1. Characteristics of RBD Palm Kernel Oil

No.	Analysis	value	
		This study	[30]
1.	Free Fatty Acid Value (as lauric acid) (%) [a]	0.05	–
2.	Water content (%) [b]	0.03	–
3.	Fatty acid composition (%) [c]		
	• Caprylic acid (C8:0)	3.57	3.24
	• Capric acid(C10:0)	3.30	3.36
	• Lauric acid (C12:0)	47.24	47.73
	• Miristic acid(C14:0)	15.18	15.91
	• Palmitic acid (C16:0)	8.80	8.25
	• Stearic acid (C18:0)	2.59	2.45
	• Oleic acid (C18:1)	15.51	15.18
4.	Slip Melting Point (°C) [d]	24.5 – 25.2	–

[a] AOCS Official Method Ca 5a-40, [b] AOCS Official Method Ca 2e-84, [c] AOCS Official Method Ce 2-66, [and d] AOCS Official Method Cc 3-25

Effect of SMS-MgO Mass Ratio on Crystallinity Index

The XRD diffraction patterns of the SMS-MgO catalyst are shown in Figure 3. Similar to Fan et al. (2013), the diffraction peaks of anhydrous Na_2SiO_3 in this catalyst mixture exhibited at 2θ angles of 17.2°, 25.4°, 29.7°, 35.4°, 37.5°, 48.4°, 52.5°, 64.6°, and 66° [36]. Conversely, the MgO diffraction peaks can be seen at 43.3° and 62.7° [42]. The peak at 43.3° is often associated with the (200) plane, and the peak at 62.7° with the (220) plane in MgO crystalline. These values can be matched with standard JCPDS (Joint Committee on Powder Diffraction Standards) cards to confirm the presence of MgO nanoparticles and their cubic structure[43]. Figure 3 demonstrates that the addition of MgO to the catalyst mixture causes several changes in peak intensity in the catalyst crystallinity profile. For example, a drop in the peak at 29.4° indicates a decrease in the degree of SMS-MgO crystallinity due to the addition of MgO. This fact can also be seen in Table 2, which shows that SMS-MgO (2.5:1) had less crystalline than other types of SMS-MgO. Magnesium oxide has a simple ionic crystal structure with alternating layers of Mg^{2+} and O^{2-} in a cubic or rock salt shape[44]. Meanwhile, sodium metasilicate crystals are silicon-oxygen tetrahedra (SiO_4) with four oxygen atoms covalently bound to each silicon (Si) atom[45]. While synthesizing the SMS-MgO catalyst, MgO particles prevented solid-to-solid interactions between sodium metasilicate particles, causing reduced catalyst crystallinity. Furthermore, it is suggested that forming an amorphous structure increases surface area of the catalyst.

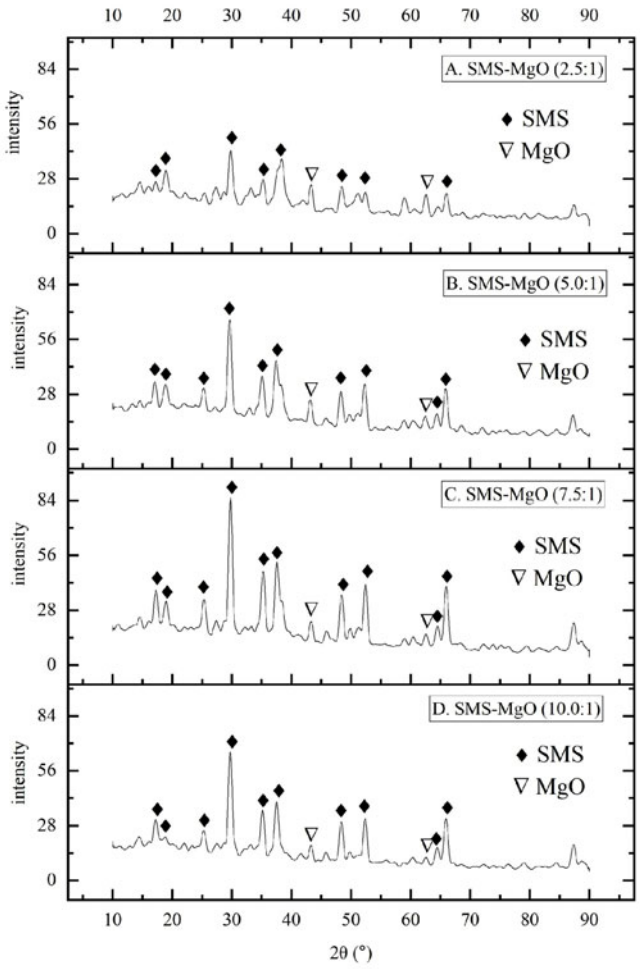

Figure 3. XRD spectrum of sodium metasilicate (SMS) to magnesium oxide (MgO) ratios. SMS-MgO ratios were 2.5:1 (A), 5.0:1 (B), 7.5:1 (C), and 10.0:1 (D)

Effect of SMS-MgO Mass Ratio on Catalyst Basicity, Surface Area, and Pore Size

The impact of the modification in the mass ratio of sodium metasilicate and MgO on the basicity of the catalyst is provided in Table 2. The catalyst basicity value increases proportionally to the amount of sodium metasilicate applied. Sodium metasilicate, with the chemical formula Na_2SiO_3, is a compound that exhibits high basicity due to the presence of silicate ions (SiO_3^{-2}). Similar to previous studies by Guo et al. and Li et al., the basicity of sodium metasilicate in this study was around 13.27 ± 0.18 mmol · g^{-1} [25, 31], and the MgO basicity value was between 0.28 and 1.18 mmol · g^{-1} [46]. Based on this observation, it can be inferred that increasing the quantity of MgO in the catalyst production procedure will reduce the basicity value within the catalyst mixture.

According to Table 2, the used catalyst has a lower basicity value than the new catalyst. The SMS-MgO (7.5:1) catalyst showed the most significant shift in base strength during the experiment. The change in the basicity value of the used catalyst was attributable to the leaching of some catalyst ions. During the glycerolysis reaction, ion exchange occurs between sodium (Na^+) and hydrogen (H^+). The absence of Na^+ ions will reduce the activity of the catalyst mixtures[47]. However, this phenomenon did not occur when using the SMS-MgO (10.0:1) catalyst. According to the data presented in Table 2, it can be observed that the basicity value of SMS-MgO (10.0:1) shows a minor drop prior to its utilization in the glycerolysis reaction. This occurs as a result of the SMS-MgO catalyst (10.0:1) agglomerating during the glycerolysis reaction. Glycerolysis processes often produce water as a byproduct through the breakdown or formation of ester bonds. In the presence of a trace quantity of water, certain Si-O-Si or Si-O-Na bonds were converted into Si-O-H bonds, forming H_4SiO_4 monomers. These monomers had the ability to conglutinate the catalyst[47]. As a result of this condition, the substrate has difficulty penetrating the catalyst lumps contained within the compartment. Hence, there was a possibility that the sodium ions contained in the catalytic mixture underwent minimal leaching and were retained within the catalyst. This solid catalyst agglomeration can reduce mass transfer efficiency and ultimately lower glycerolysis yield[17].

Based on Table 2, the SMS-MgO catalyst has micro--size pores (less than 2 nm). The SMS-MgO catalyst with a ratio of 5.0:1 exhibits a particularly smaller pore size compared to other SMS-MgO catalysts. In addition to this, the SMS-MgO (5.0:1) catalyst exhibits an increased surface area. Due to the amorphous nature of MgO, the addition of MgO to the catalytic mixture will affect expanding the surface area of the catalyst. Even though the SMS-MgO (10.0:1) catalyst exhibits a greater pore size in comparison to the SMS-MgO (5.0:1) catalyst, it is noticeable that the SMS-MgO (10.0:1) possesses a smaller pore volume, resulting in a lower surface area.

Effect of Catalyst on pH Value of Glycerolysis Product

In this research, we observed the effect of utilizing catalysts with varying mass ratios of sodium metasilicate

Table 2. Effect of Sodium Metasilicate and MgO Mass Ratio on Basicity, Surface Area, Pore Volume, and Pore Size of Catalyst

Catalyst	Basicity (mmol · g^{-1})		Surface area ($m^2 \cdot g^{-1}$)	Pore volume ($cm^3 \cdot g^{-1}$)	Pore size (nm)	Crystallinity Index
	new	used				
SMS-MgO (2.5:1)	9.07 ± 0.095[a]	8.03 ± 0.092[a]	3.99	0.0031	1.53	21.14
SMS-MgO (5.0:1)	11.59 ± 0.115[b]	8.56 ± 0.017[a]	4.22	0.0030	1.41	24.76
SMS-MgO (7.5:1)	12.32 ± 0.073[c]	7.56 ± 0.690[a]	3.91	0.0035	1.79	29.21
SMS-MgO (10.0:1)	13.25 ± 0.021[d]	12.32 ± 0.753[b]	2.12	0.0018	1.67	24.89

Glycerolysis reaction: time 360 min; catalyst loading 20 wt% (mass of oil); agitation speed 2000 rpm; temperature 120 °C
Different letters indicated significantly different values for each column ($p < 0.05$)

and MgO on the final product's pH value. As shown in Table 3, the SMS-MgO (5.0:1) catalyst produced a product with the highest pH value of 9.42 ± 0.15. During glycerolysis process, the sodium metasilicate catalyst will react with the water formed by the reaction. Sodium metasilicate is an alkaline chemical that produces silicate ions when dissolved in water, which can combine with water to form silicic acid. In the presence of water, sodium metasilicate hydrolysis results in NaOH and Si-O-H[47].

The increase in pH value of the product was likely affected by NaOH molecules produced during the reaction process. The glycerolysis reaction can be accelerated by NaOH molecules that are produced during sodium metasilicate hydrolysis[47]. The presence of NaOH in the substrate will assist in initiating the interesterification process that occurs in acylglycerol. In addition, it is also believed that the formation of glycerolate anion during the glycerolysis reaction is responsible for the increase in the pH of the product. Anion glycerolate usually forms in ionic liquid solvents, which are liquid salts made of ions. These parts are very soluble in glycerol and other reactants and exhibit strong polarity. The higher solubility of reactants in anion glycerolate promotes effective collisions and increases the reaction rate. Glycerolate's negative charge also stabilizes the reaction intermediate. This stabilization will decrease the energy barrier, making the reaction easier and faster[48].

Effect of Catalyst on TAG Conversion

In glycerolysis processes, heterogeneous catalysts aim to obtain a form of catalyst that can be readily separated and recycled for additional usage. The primary objective was to maximize the rate at which TAGs can be converted into MAG and DAG. The glycerolysis reaction proceeds in two sequential stages: initially, TAG reacts with glycerol to form MAG and DAG (Eq. 5 and Eq. 6), and subsequently, DAG further reacts with glycerol to produce additional MAG (Eq. 7)[1, 8]. Several studies have been conducted to determine the most effective heterogeneous catalyst for this glycerolysis process. It has been mentioned in various published works that the conversion rate of TAG into MAG and DAG is increased according to the basicity value of the heterogeneous catalyst that is utilized[14, 25].

$$\text{TAG} + \text{Gly} \leftrightarrow \text{MAG} + \text{DAG} \quad (5)$$

$$\text{TAG} + 2\text{Gly} \leftrightarrow 3\text{MAG} \quad (6)$$

$$\text{DAG} + \text{Gly} \leftrightarrow 2\text{MAG} \quad (7)$$

According to the research, heterogeneous catalysts with extremely high basicity values may not always give the greatest TAG conversion. Figure 4 shows that the glycerolysis reaction with the SMS-MgO (10.0:1) catalyst, which has the highest basicity value, has a lower TAG conversion rate than the glycerolysis reaction with the SMS-MgO (5.0:1) catalyst. This phenomenon occurs due to the tendency of catalysts containing large quantities of sodium metasilicate to agglomerate. Furthermore, the SMS-MgO (10.0:1) catalyst was known to have a lower value than the SMS-MgO (5.0:1) catalyst based on the measurement of the surface area of the catalyst using the BET technique (Table 2). There is a correlation between crystallinity and catalytic activity in specific situations. Siregar et al. found that a crystalline phase of

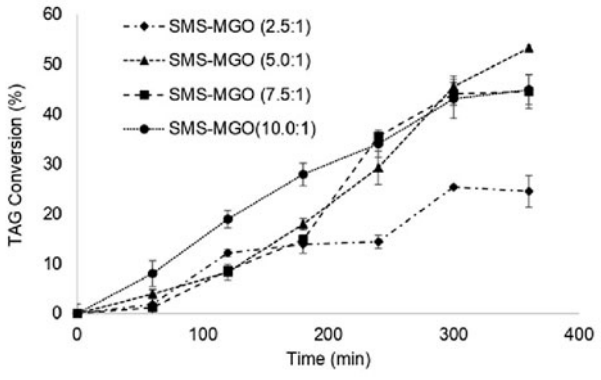

Figure 4. Effect of various catalysts on the TAG conversion. Reactions were performed at RBDPKO/Gly molar ratio 1:3; temperature 120 °C; catalyst loading 20 wt%; time 360 min; agitation speed 2000 rpm

Table 3. Effect of Sodium Metasilicate/MgO Mass Ratio on pH Value and Acylglycerol Composition in The Product

Catalyst	pH value	Acylglycerol (%)		TAG conversion (%)
		MAG	DAG	
SMS-MgO (2.5:1)	7.83±0.11[a]	3.61 ± 0.440[a]	21.09 ± 2.555[a]	24.55 ± 3.157[a]
SMS-MgO (5.0:1)	9.42±0.15[b]	17.03 ± 0.475[b]	36.21 ± 1.723[b]	53.04 ± 2.152[c]
SMS-MgO (7.5:1)	9.20±0.47[b]	14.29 ± 3.086[b]	30.36 ± 1.502[b]	44.54 ± 3.402[bc]
SMS-MgO (10.0:1)	9.34±0.23[b]	8.24 ± 1.888[a]	35.45 ± 1.238[b]	43.58 ± 3.116[b]

Glycerolysis reaction: time 360 min; catalyst loading 20 wt% (mass of oil); agitation speed 2000 rpm; temperature 120 °C
Different letters indicated significantly different values for each column ($p < 0.05$)

the sodium silicate catalyst was formed by impregnating NaOH onto calcined silica corncob ash[23]. The results showed that a catalyst with a high degree of crystallinity was more active than the amorphous ones. Crystalline materials have enhanced surface reactivity due to their regular atom arrangement. A crystal's surface atoms are closer to reactant molecules, causing catalytic reactions more effective. Nonetheless, the increased surface area of amorphous catalysts allows them to outperform their crystalline counterparts in terms of activity. SMS-MgO (5.0:1) catalyst has a larger surface area (4.22 $m^2 \cdot g^{-1}$) allowing for more interactions between the reactant and the catalyst, leading to enhanced catalytic activity.

Effect of Catalyst on Acylglycerols

As previously mentioned, the SMS-MgO (5.0:1) catalyst generates products with the greatest pH values. Glycerolate anion can arise in substrate mixtures due to strong catalytic activity. It allows high-MAG and DAG products, as demonstrated in Table 3. As seen in Figure 5, the glycerolysis reaction carried out using SMS--MgO (5.0:1) and (7.5:1) catalysts produced a significant increase in MAG and DAG after 180 min. Meanwhile, a significant decrease in TAG occurred in the SMS-MgO (10.0:1) catalyst in the 60th min. After that, TAG levels tended to remain steady or did not decrease much. Due to the low basicity, the SMS-MgO (2.5:1) catalyst was insufficient to react with the substrate attached to the catalyst's surface. As a result, this catalyst could not convert TAG significantly.

Additionally, the physical characteristics of the catalyst show an effect on the rate of conversion of triacylglycerol (TAG) into monoacylglycerol (MAG) and diacylglycerol (DAG). Increasing the catalyst's surface area will enhance the interaction between the substrate and the catalyst. Using SMS-MgO (5.0:1) as a catalyst, characterized by its substantial surface area, leads to an enhanced production yield of MAG and DAG molecules (17.03±0.475 and 36.21±1.723%, respectively). The accessibility and transport of chemicals that interact on the catalyst's surface are influenced by the catalyst's pore size and pore volume[49].

CONCLUSION

The production of MAG and DAG products using RBDPKO oil as feedstock has been successfully achieved using a mixture of catalysts derived from SMS and MgO in a HSCR. Based on the evaluation of the catalyst characteristics, SMS contained Si-O-Si stretching and the O-Si-O bonds. Impregnation of SMS with MgO reduced the O-Si-O bonds and increased Mg-O-Mg stretching and Mg-O bond vibrations. The MgO particles prevented solid-solid interactions between the SMS particles, resulting in reduced catalyst crystallinity. SMS basisity was about 13.27 ± 0.18 mmol · g^{-1}. Increasing the amount of MgO in the SMS-MgO catalyst reduced its basicity value (0.28–1.18 mmol · g^{-1}). In addition, the SMS-MgO catalyst had micro-sized pores (less than 2 nm). SMS--MgO (10.0:1) catalyst had a lower surface area than the SMS-MgO (5.0:1) catalyst. The increase in surface area was due to the amorphous nature of MgO.

Based on the catalyst activity evaluation, SMS-MgO (5.0:1) increased the MAG and DAG production yields (17.03±0.475 and 36.21±1.723%, respectively). This is due to the increased surface area (4.22 m2 · g^{-1}) and the formation of NaOH and Si-O-H from the hydrolysis of SMS during the glycerolysis reaction. The product pH was 9.42±0. On the other hand, SMS-MgO (10.0:1) had the highest basicity value, but the catalyst activity was lower than SMS-MgO (5.0:1). This is due to the agglomeration of the SMS-MgO (10.0:1) catalyst. Thus, MgO potentially prevents the formation of O-Si-O bonds, forms an amorphous structure, increases the surface area of the catalyst and minimises catalyst agglomeration. Finally, it improves their catalytic activity.

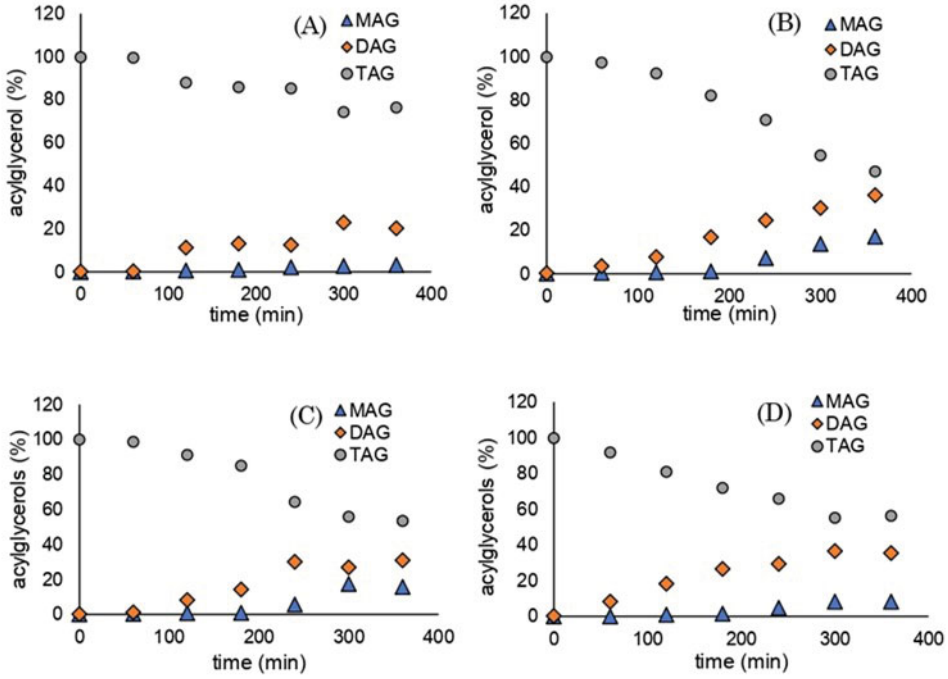

Figure 5. Effect of sodium metasilicate (SMS) to magnesium oxide (MgO) ratios on acylglycerol compositions. SMS-MgO ratios were 2.5:1 (A), 5.0:1 (B), 7.5:1 (C) and 10.0:1 (D)

ACKNOWLEDGEMENT

The authors are grateful to the Directorate of General Education, Ministry of Education and Culture, Indonesia, who kindly provided all funding for this study through the doctor's dissertation research scheme (number of contract agreements: 122/E5/PG.02.00.PL/2023 and 3121/UN1/DITLIT/Dit-Lit/PT.01.03/2023).

LITERATURE CITED

1. Alvarez Serafini, M.S. & Tonetto, G.M. (2019). Catalytic Synthesis of Monoglycerides by Glycerolysis of Triglycerides. *Internat. J. Chem. Reactor Engin*. 17(11). DOI: 10.1515/ijcre-2019-0056.

2. Buchori, L., Anggoro, D.D., Sumantri, I. & Putra, R.R.R. (2019). Optimization of monoglycerides production using KF/CaO-MgO heterogeneous catalysis. *Bull. Chemical Reaction Engin. Catalysis*. 14(3), 689–696. DOI: 10.9767/bcrec.14.3.4251.689-696.

3. Zha, B., Chen, Z., Wang, L., Wang, R., Chen, Z. & Zheng, L. (2014). Production of glycerol monolaurate-enriched monoacylglycerols by lipase-catalyzed glycerolysis from coconut oil. *Europ. J. Lipid Sci. Technol*. 116(3), 328–335. DOI: 10.1002/ejlt.201300243.

4. Vilas Bôas, R.N., Lima, R., Silva, M.V.C., Freitas, L., Aguiar, L.G. & de Castro, H.F. (2021). Continuous production of monoacylglycerol via glycerolysis of babassu oil by immobilized Burkholderia cepacia lipase in a packed bed reactor. *Bioproc. Biosyst. Eng*. 44(10), 2205–2215. DOI: 10.1007/s00449-021-02596-6.

5. Arum, A., Hidayat, C. & Supriyanto. (2019). Synthesis of Emulsifier from Refined Bleached Deodorized Palm Stearin by Chemical Glycerolysis in Stirred Tank Reactor. KnE Life Sci. 4(11), 130. DOI: 10.18502/kls.v4i11.3859.

6. Cerro-Alarcón, M., Corma, A., Iborra, S., Martínez, C. & Sabater, M.J. (2010). Methanolysis of sunflower oil using gem-diamines as active organocatalysts for biodiesel production. *Appl. Catal. A Gen*. 382(1), 36–42. DOI: 10.1016/j.apcata.2010.04.024.

7. Laskar, I.B., Changmai, B., Gupta, R., Shi, D., Jenkinson, K.J., Wheatley, A.E.H. & Rokhum, S.L. (2021). A mesoporous polysulfonic acid-formaldehyde polymeric catalyst for biodiesel production from Jatropha curcas oil. *Renew Energy*. 173, 415–421. DOI: 10.1016/j.renene.2021.04.004.

8. Zhong, N., Li, L., Xu, X., Cheong, L.Z., Xu, Z. & Li, B. (2013). High yield of monoacylglycerols production through low-temperature chemical and enzymatic glycerolysis. *Europ. J. Lipid Sci. Technol*. 115(6), 684–690. DOI: 10.1002/ejlt.201200377.

9. Coman, S.M. & Parvulescu, V.I. Published online 2013. Heterogeneous Catalysis for Biodiesel Production. *The Role of Catalysis for the Sustainable Production of Bio-Fuels and Bio--Chemicals*. 93–136. DOI: 10.1016/B978-0-444-56330-9.00004-8.

10. Navas, M.B., Ruggera, J.F., Lick, I.D. & Casella, M.L. (2020). A sustainable process for biodiesel production using Zn/Mg oxidic species as active, selective and reusable heterogeneous catalysts. *Biores. Bioprocess*. 7(1). DOI: 10.1186/s40643-019-0291-3.

11. Lee, H.V., Juan, J.C., Yun Hin, T.Y. & Ong, H.C. (2016). Environment-friendly heterogeneous alkaline-Based mixed metal oxide catalysts for biodiesel production. *Energies (Basel)* 9(8). DOI: 10.3390/en9080611.

12. Mostafa, N.A., Maher, A. & Abdelmoez, W. (2013). Production of mono-, di-, and triglycerides from waste fatty acids through esterification with glycerol. *Adv. Biosc. Biotechnol*. 4(09), 900–907. DOI: 10.4236/abb.2013.49118.

13. Belelli, PG.G., Ferretti, CA.A., Apesteguía, CR.R., Ferullo, RM.M. & Di Cosimo, JI.I. (2015). Glycerolysis of methyl oleate on MgO: Experimental and theoretical study of the reaction selectivity. *J. Catal*. 323, 132–144. DOI: 10.1016/j.jcat.2015.01.001.

14. Wangi, I.P., Supriyanto, S., Sulistyo, H. & Hidayat, C. (2022). Sodium Silicate Catalyst for Synthesis Monoacylglycerol and Diacylglycerol-Rich Structured Lipids : Product Characteristic and Glycerolysis – Interesterification Kinetics. 17(2). DOI: 10.9767/bcrec.17.2.13306.250-262.

15. Ye, B., Qiu, F., Sun, C., Li, Y. & Yang, D. (2014). Biodiesel production from soybean oil using heterogeneous solid base catalyst. *J. Chem. Technol. Biotech*. 89(7), 988–997. DOI: 10.1002/jctb.4190.

16. Prabu, M., Manikandan, M., Kandasamy, P., Kalaivani, P.R., Rajendiran, N. & Raja, T. (2019). Synthesis of Biodiesel using the Mg/Al/Zn Hydrotalcite/SBA-15 Nanocomposite Catalyst. *ACS Omega*. 4(2), 3500–3507. DOI: 10.1021/acsomega.8b02547.

17. Chen, Y.C., Lin, D.Y. & Chen, B.H. (2019). Metasilicate-based catalyst prepared from natural diatomaceous earth for biodiesel production. *Renew Energy*. 138, 1042–1050. DOI: 10.1016/j.renene.2019.02.054.

18. Nguyen-Phu, H., Park, C.-yi. & Eun, W.S. (2016). Activated red mud-supported Zn/Al oxide catalysts for catalytic conversion of glycerol to glycerol carbonate: FTIR analysis. *Catal. Commun*. 85(3), 52–56. DOI: 10.1016/j.catcom.2016.07.012.

19. Jagadeeswaraiah, K., Kumar, C.R., Prasad, P.S.S., Loridant, S. & Lingaiah, N. (2014). Synthesis of glycerol carbonate from glycerol and urea over tin-tungsten mixed oxide catalysts. *Appl. Catal. A Gen*. 469, 165–172. DOI: 10.1016/j.apcata.2013.09.041.

20. Sulistyo, H., Sediawan, W.B., Suyatmo, R.I.D. & Hartati, I. (2021). Kinetic studies of the glycerolysis of urea to glycerol carbonate in the presence of amberlyst-15 as catalyst. *Bull. Chem. Reaction Engin. Catal.* 16(1), 52–62. DOI: 10.9767/BCREC.16.1.8893.52-62.

21. Konwar, L.J., Mäki-Arvela, P., Kumar, N., et al. (2016). Selective esterification of fatty acids with glycerol to monoglycerides over –SO3H functionalized carbon catalysts. *Reaction Kinet. Mech. Catal*. 119(1), 121–138. DOI: 10.1007/s11144-016-1040-7.

22. Zhang, S., Fu, J., Xing, S., Li, M., Liu, X., Yang, L. & Lv, P. (2023). Sodium Silicates Modified Calcium Oxide as a High-Performance Solid Base Catalyst for Biodiesel Production. *Catalysts*. 13(4), 775. DOI: 10.3390/catal13040775.

23. Siregar, A.G.A., Manurung, R. & Taslim, T. (2021). Synthesis and characterization of sodium silicate produced from corncobs as a heterogeneous catalyst in biodiesel production. *Indonesian J. Chem*. 21(1), 88–96. DOI: 10.22146/ijc.53057.

24. Ferretti, C.A., Apesteguía, C.R. & Di Cosimo, J.I. (2011). MgO-based catalysts for monoglyceride synthesis from methyl oleate and glycerol: Effect of Li promotion. *Appl. Catal. A Gen*. 399(1–2), 146–153. DOI: 10.1016/j.apcata.2011.03.051.

25. Guo, F., Peng, Z.G., Dai, J.Y. & Xiu, Z.L. (2010). Calcined sodium silicate as solid base catalyst for biodiesel production. *Fuel Proces. Technol*. 91(3), 322–328. DOI: 10.1016/j.fuproc.2009.11.003.

26. Fallah Kelarijani, A., Gholipour Zanjani, N., Kamran Pirzaman, A., Kelarijani, A., Zanjani, N. & Pirzaman, A. (2020). Ultrasonic Assisted Transesterification of Rapeseed Oil to Biodiesel Using Nano Magnetic Catalysts. *Waste Biomass Valorization*. 11(6), 2613–2621. DOI: 10.1007/s12649-019-00593-1.

27. Pithani, S., Karlsson, S., Emtenäs, H. & Öberg, C.T. (2019). Using Spinchem Rotating Bed Reactor Technology for Immobilized Enzymatic Reactions: A Case Study. *Org Process Res Dev*. 23(9), 1926–1931. DOI: 10.1021/acs.oprd.9b00240.

28. de Oliveira, K.G., de Lima, R.R.S., de Longe, C., de C. Bicudo, T., Sales, R. V., de Carvalho, L.S., Oliveira, K.G. De., Lima, R.R.S. De. & Longe, C. De. (2022). Sodium and potassium silicate-based catalysts prepared using sand silica concerning biodiesel production from waste oil. *Arabian J. Chem*. 15(2), 103603. DOI: 10.1016/j.arabjc.2021.103603.

29. Brunauer, S., Emmett, P.H. & Teller, E. (1938). Adsorption of Gases in Multimolecular Layers. *J. Am. Chem. Soc*. 60(2), 309–319. DOI: 10.1021/ja01269a023.

30. Barrett, E.P., Joyner, L.G. & Halenda, P.P. (1951). The Determination of Pore Volume and Area Distributions in Porous Substances. I. Computations from Nitrogen Isotherms. *J. Am. Chem. Soc*. 73(1), 373–380. DOI: 10.1021/ja01145a126.

31. Li, B., Li, H., Zhang, X., Fan, P., Liu, L., Li, B., Dong, W. & Zhao, B. (2019). Calcined sodium silicate as an efficient and benign heterogeneous catalyst for the transesterification of natural lecithin to L-α-glycerophosphocholine. *Green Proces. Synthesis*. 8(1), 78–84. DOI: 10.1515/gps-2017-0190.

32. AOCS. Published online 2009. AOCS Ca 5a-40 Free Fatty Acids. In: *Official Methods and Recommended Practices of the American Oil Chemist's Society*. 2009. https://myaccount.aocs.org/PersonifyEbusiness/Store/Product-Details?productId=111480

33. Subroto, E., Wisamputri, M.F., Supriyanto., Utami, T. & Hidayat, C. (2020). Enzymatic and chemical synthesis of high mono- and diacylglycerol from palm stearin and olein blend at different type of reactor stirrers. *J. Saudi Soc. Agric. Sci*. 19(1), 31–36. DOI: 10.1016/j.jssas.2018.05.003.

34. Kılıç, B. & Özer, C.O. (2019). Potential use of interesterified palm kernel oil to replace animal fat in frankfurters. *Meat Sci*. 148(October 2018), 206–212. DOI: 10.1016/j.meatsci.2018.08.024.

35. Sun, Z., Duan, X., Srinivasakannan, C. & Liang, J. (2018). Preparation of magnesium silicate/carbon composite for adsorption of rhodamine B. *RSC Adv*. 8(14), 7873–7882. DOI: 10.1039/c7ra12848g.

36. Fan, F., Jia, L., Guo, X., Lu, X. & Chen, J. (2013). Preparation of novel ethylene glycol monomethyl ether fatty acid monoester biodiesel using calcined sodium silicate. *Energy and Fuels*. 27(9), 5215–5221. DOI: 10.1021/ef401514e.

37. Gliński, M., Iwanek Nee Wilczkowska, E.M., Ulkowska, U., Czajka, A. & Kaszkur, Z. (2021). Catalytic activity of high-surface-area amorphous mgo obtained from upsalite. *Catalysts* 11(11), 1–14. DOI: 10.3390/catal11111338.

38. Zahir, M.H., Rahman, M.M.M., Irshad, K. & Rahman, M.M.M. (2019). Shape-stabilized phase change materials for solar energy storage: MgO and mg(OH)2 mixed with polyethylene glycol. *Nanomaterials* 9(12), 1–21. DOI: 10.3390/nano9121773.

39. Gao, X., Asgar, H., Kuzmenko, I. & Gadikota, G. (2021). Architected mesoporous crystalline magnesium silicates with ordered pore structures. *Microp. Mesop. Mater*. 327,. DOI: 10.1016/j.micromeso.2021.111381.

40. Manríquez-Ramírez, M., Gómez, R., Hernández-Cortez, J.G., Zúñiga-Moreno, A., Reza-San Germán, C.M. & Flores-Valle, S.O. (2013). Advances in the transesterification of triglycerides to biodiesel using MgO–NaOH, MgO–KOH and MgO–CeO2 as solid basic catalysts. *Catal Today*. 212, 23–30. DOI: 10.1016/j.cattod.2012.11.005.

41. Balakrishnan, G., Velavan, R., Mujasam Batoo, K. & Raslan, E.H. (2020). Microstructure, optical and photocatalytic properties of MgO nanoparticles. *Results Phys*. 16(February), 103013. DOI: 10.1016/j.rinp.2020.103013.

42. Stefanidis, S.D., Karakoulia, S.A., Kalogiannis, K.G., Iliopoulou, E.F., Delimitis, A., Yiannoulakis, H., Zampetakis, T., Lappas, A.A. & Triantafyllidis, K.S. (2016). Natural magnesium oxide (MgO) catalysts: A cost-effective sustainable alternative to acid zeolites for the in situ upgrading of biomass fast pyrolysis oil. *Appl. Catal. B*. 196, 155–173. DOI: 10.1016/j.apcatb.2016.05.031.

43. Singh, N., Singh, P.K., Shukla, A., Singh, S. & Tandon, P. (2016). Synthesis and Characterization of Nanostructured Magnesium Oxide: Insight from Solid-State Density Functional Theory Calculations. *J. Inorg. Organomet. Polym. Mater*. 26(6), 1413–1420. DOI: 10.1007/s10904-016-0411-x.

44. Di Cosimo, J.I., Díez, V.K., Ferretti, C. & Apesteguía, C.R. (2014). Basic catalysis on MgO: Generation, characterization and catalytic properties of active sites. *Catalysis* 26(3000), 1–28. DOI: 10.1039/9781782620037-00001.

45. Kahlenberg, V. (2010). Structural chemistry of anhydrous sodium silicates - A review. *Chimia (Aarau)*. 64(10), 716–722. DOI: 10.2533/chimia.2010.716.

46. Anggoro, D.D., Buchori, L., Sasongko, S.B. & Oktavianty, H. (2019). Basicity Optimization of KF/Ca-MgO Catalyst using Impregnation Method. *Bull. Chem. Reaction Engin. Catal*. 14(3), 678–682. DOI: 10.9767/bcrec.14.3.4248.678-682.

47. Guo, F., Wei, N.N., Xiu, Z.L. & Fang, Z. (2012). Transesterification mechanism of soybean oil to biodiesel catalyzed by calcined sodium silicate. *Fuel*. 93, 468–472. DOI: 10.1016/j.fuel.2011.08.064.

48. Dijkstra, A.J. (2020). Some Thoughts on the Mechanism of Ester Interchange Reactions Involving Acylglycerols. *Europ. J. Lipid Sci. Technol*. 122(10), 2000188. DOI: 10.1002/ejlt.202000188.

49. Botti, R.F., Innocentini, M.D.M., Faleiros, T.A., Mello, M.F., Flumignan, D.L., Santos, L.K., Franchin, G. & Colombo, P. (2020). Biodiesel Processing Using Sodium and Potassium Geopolymer Powders as Heterogeneous Catalysts. *Molecules* 25(12). DOI: 10.3390/molecules25122839.